

Fluorescence enhancement by a two-dimensional dielectric annular Bragg resonant cavity

Yongmin Liu,^{1,3} Sheng Wang,^{1,3} Yong-Shik Park,^{1,3} Xiaobo Yin,^{1,2} and Xiang Zhang^{1,2,*}

¹*NSF Nanoscale Science and Engineering Center (NSEC), 3112 Etcheverry Hall,
University of California, Berkeley, CA 94720, USA*

²*Materials Sciences Division, Lawrence Berkeley National Laboratory, 1 Cyclotron Road,
Berkeley, CA 94720, USA*

³ *These authors contributed equally to this work*

* xiang@berkeley.edu

Abstract: We show that photons can be efficiently extracted from fluorescent molecules, utilizing the strongly enhanced local field of a two-dimensional dielectric annular Bragg resonant cavity. Due to the diffraction and constructive interference together with the annular focusing, the periodic ring structure converts the normal incident light into planar guided modes and forms a hot spot at the center of the structure. Theoretically, the field can be enhanced more than 40 times, which leads to the averaged 20-fold enhancement of the fluorescence signal observed in experiments. Compared with fluorescence enhancement by plasmonic structures, this dielectric approach does not suffer from pronounced quenching that often occurs near metallic structures. These results not only can be applied as ultrasensitive sensors for various biological systems, but also have broad potential applications, such as optical trapping and fluorescent microscopy.

©2010 Optical Society of America

OCIS codes: (300.2530) Fluorescence, laser-induced; (310.6628) Subwavelength structures, nanostructures ; (260.5740) Resonance.

References and links

1. G. W. Ford, and W. H. Weber, "Electromagnetic interactions of molecules with metal surfaces," *Phys. Rep.* **113**(4), 195–287 (1984).
2. E. Fort, and S. Grésillon, "Surface enhanced fluorescence," *J. Phys. D Appl. Phys.* **41**(1), 013001 (2008).
3. F. D. Stefani, K. Vasilev, N. Bocchio, N. Stoyanova, and M. Kreiter, "Surface-plasmon-mediated single-molecule fluorescence through a thin metallic film," *Phys. Rev. Lett.* **94**(2), 023005 (2005).
4. Y. J. Hung, I. I. Smolyaninov, C. C. Davis, and H. C. Wu, "Fluorescence enhancement by surface gratings," *Opt. Express* **14**(22), 10825–10830 (2006).
5. P. Anger, P. Bharadwaj, and L. Novotny, "Enhancement and quenching of single-molecule fluorescence," *Phys. Rev. Lett.* **96**(11), 113002 (2006).
6. F. Tam, G. P. Goodrich, B. R. Johnson, and N. J. Halas, "Plasmonic enhancement of molecular fluorescence," *Nano Lett.* **7**(2), 496–501 (2007).
7. A. Kinkhabwala, Z. Yu, S. Fan, Y. Avlasevich, K. Mullen, and W. E. Moerner, "Single-molecule fluorescence enhancements produced by a Bowtie nanoantenna," *Nat. Photonics* **3**(11), 654–657 (2009).
8. S. Wang, D. F. P. Pile, C. Sun, and X. Zhang, "Nanopin plasmonic resonator array and its optical properties," *Nano Lett.* **7**(4), 1076–1080 (2007).
9. V. G. Kravets, G. Zoriniants, C. P. Burrows, F. Schedin, A. K. Geim, W. L. Barnes, and A. N. Grigorenko, "Composite au nanostructures for fluorescence studies in visible light," *Nano Lett.* **10**(3), 874–879 (2010).
10. S. S. Wang, and R. Magnusson, "Theory and applications of guided-mode resonance filters," *Appl. Opt.* **32**(14), 2606–2613 (1993).
11. M. Boroditsky, T. F. Krauss, R. Coccioli, R. Virjen, R. Bhat, and E. Yablonovitch, "Light extraction from optically pumped light-emitting diode by thin-slab photonic crystals," *Appl. Phys. Lett.* **75**(8), 1036–1038 (1999).
12. M. Laroche, S. Albaladejo, R. Carminati, and J. J. Sáenz, "Optical resonances in one-dimensional dielectric nanorod arrays: field-induced fluorescence enhancement," *Opt. Lett.* **32**(18), 2762–2764 (2007).
13. N. Ganesh, W. Zhang, P. C. Mathias, E. Chow, J. A. N. T. Soares, V. Malyarchuk, A. D. Smith, and B. T. Cunningham, "Enhanced fluorescence emission from quantum dots on a photonic crystal surface," *Nat. Nanotechnol.* **2**(8), 515–520 (2007).
14. N. Ganesh, I. D. Block, P. C. Mathias, W. Zhang, E. Chow, V. Malyarchuk, and B. T. Cunningham, "Leaky-mode assisted fluorescence extraction: application to fluorescence enhancement biosensors," *Opt. Express* **16**(26), 21626–21640 (2008).

15. P. Karvinen, T. Nuutinen, O. Hyvärinen, and P. Vahimaa, "Enhancement of laser-induced fluorescence at 473 nm excitation with subwavelength resonant waveguide gratings," *Opt. Express* **16**(21), 16364–16370 (2008).
16. U. Becherer, T. Moser, W. Stühmer, and M. Oheim, "Calcium regulates exocytosis at the level of single vesicles," *Nat. Neurosci.* **6**(8), 846–853 (2003).
17. J. N. Anker, W. P. Hall, O. Lyandres, N. C. Shah, J. Zhao, and R. P. Van Duyne, "Biosensing with plasmonic nanosensors," *Nat. Mater.* **7**(6), 442–453 (2008).
18. M. Righini, P. Ghenuche, S. Cherukulappurath, V. Myroshnychenko, F. J. García de Abajo, and R. Quidant, "Nano-optical trapping of Rayleigh particles and Escherichia coli bacteria with resonant optical antennas," *Nano Lett.* **9**(10), 3387–3391 (2009).
19. A. N. Grigorenko, N. W. Roberts, M. R. Dickinson, and Y. Zhang, "Nanometric optical tweezers based on nanostructured substrates," *Nat. Photonics* **2**(6), 365–370 (2008).
20. M. J. Levene, J. Korch, S. W. Turner, M. Foquet, H. G. Craighead, and W. W. Webb, "Zero-mode waveguides for single-molecule analysis at high concentrations," *Science* **299**(5607), 682–686 (2003).
21. J. Scheuer, and A. Yariv, "Annular Bragg defect mode resonators," *J. Opt. Soc. Am. B* **20**(11), 2285 (2003).
22. J. Scheuer, W. M. J. Green, G. A. DeRose, and A. Yariv, "Lasing from a circular Bragg nanocavity with an ultrasmall modal volume," *Appl. Phys. Lett.* **86**(25), 251101 (2005).
23. R. W. Wood, "On a remarkable case of uneven distribution of light in a diffraction grating spectrum," *Philos. Mag.* **4**, 392–402 (1902).
24. S. S. Wang, R. Magnusson, J. S. Bagby, and M. G. Moharam, "Guided-mode resonances in planar dielectric-layer diffraction gratings," *J. Opt. Soc. Am. A* **7**(8), 1470–1474 (1990).
25. Q. F. Xu, V. R. Almeida, R. R. Panepucci, and M. Lipson, "Experimental demonstration of guiding and confining light in nanometer-size low-refractive-index material," *Opt. Lett.* **29**(14), 1626–1628 (2004).
26. Ö. Duyar, F. Placido, and H. Z. Durusoy, "Optimization of TiO₂ films prepared by reactive electron beam evaporation of Ti₃O₅," *J. Phys. D Appl. Phys.* **41**(9), 095307 (2008).
27. V. G. Kravets, F. Schedin, and A. N. Grigorenko, "Extremely narrow plasmon resonances based on diffraction coupling of localized plasmons in arrays of metallic nanoparticles," *Phys. Rev. Lett.* **101**(8), 087403 (2008).

1. Introduction

Fluorescent molecules have many applications, including fluorescence microscopy and biological sensing. To achieve fluorescence detection with a high signal-to-noise ratio, it is highly desirable to extract more photons from fluorescent molecules, and let them efficiently radiate into the far field. Extensive effort has been made towards this goal. For instance, using the strong near-field enhancement of surface plasmon modes, people have demonstrated that the fluorescence emission can be improved up to three orders of magnitude [1–9]. However, if fluorescent molecules are very close to the metal surface (usually within tens of nanometers), a large amount of energy emitted by the molecules will undergo the plasmon mode and lossy surface wave channels. Eventually energy dissipates into heat due to the intrinsic Ohmic loss of metals, that is, the fluorescence is quenched [1,2,5]. Therefore, it is critical to balance the increase of the local field intensity and the reduction of the external quantum yield, so that the fluorescence can be effectively enhanced. On the other hand, it is found that purely dielectric structures, such as one-dimensional (1D) periodic gratings or two-dimensional (2D) photonic crystals, can also produce substantial local field enhancement thanks to the resonant photonic modes of the dielectric system [10–15]. Such a platform based on sole dielectrics normally exhibits much less losses in the optical region compared to plasmonic structures. Thus fluorescence signals can be enhanced without suffering from pronounced quenching.

However, so far 1D or 2D periodic dielectric structures have not shown confined fluorescence emission. In other words, macroscopically the fluorescence is amplified over the entire space of the periodically structured dielectrics. Under some conditions, we may want to selectively choose a certain area, sometimes a small one, to locally enhance fluorescence emission and use it for subcellular biosensing applications [16,17]. Here we demonstrate that based on a 2D dielectric annular Bragg resonator, electromagnetic waves can be focused to a diffraction-limited spot and significantly boost the fluorescence emission. Experimentally we observe 20-fold fluorescence enhancement averaged over an area of 4 μm^2 , while theoretically the fluorescence emission can be increased by more than three orders of magnitude at the central point of the resonator. These findings could be very useful for biosensor applications which are particularly interesting for biological sensing down to subcellular level [16]. Not limited in sensing, such a strongly enhanced local field can also be utilized for near-field optical trapping and manipulation [18,19]. Our demonstration in this work may also have potential applications for fluorescence microscopy, and fluorescence

correlation spectroscopy (FCS) at the single-molecule level [20], where the individual target molecules can diffuse in and out of the strong field-enhancement region to give the flashes of signals.

2. Field enhancement in annular Bragg resonators

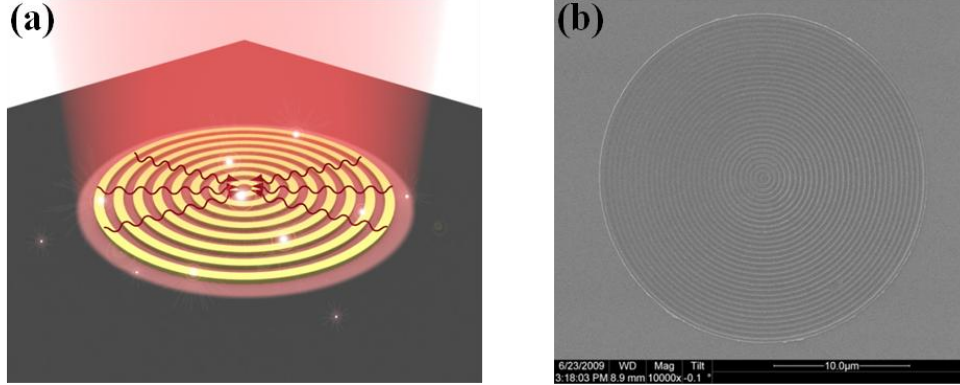


Fig. 1. (a) Schematic of the annular Bragg resonator. The perpendicular incident waves are converted to in-plane resonant guided modes, and focused at the center of the cavity. Consequently, fluorescence emission is enhanced. (b) Scanning electron microscope (SEM) image of one fabricated annular Bragg resonator.

It is well known that the fluorescence emission is given by [5]

$$\gamma_{em} = \gamma_{exc} \cdot \eta_{ext} \quad (1)$$

In Eq. (1), the excitation rate γ_{exc} is proportional to $|\vec{p} \cdot \vec{E}|^2$, where \vec{p} is the transition dipole moment of a fluorophore and \vec{E} is the local excitation field (incident plus scattered). Assuming the internal quantum efficiency of the fluorophore is unity, then the formula for the external quantum efficiency is

$$\eta_{ext} = \gamma_{rad} / (\gamma_{rad} + \gamma_{non-rad}) \quad (2)$$

where γ_{rad} and $\gamma_{non-rad}$ represent the radiative and non-radiative enhancement factor, respectively. If the non-radiative channel is more dominant than the far-field radiation channel due to the strong coupling between the emitted photons and the plasmon mode or lossy surface wave, the external quantum efficiency can significantly compromise the effect of the local field enhancement on the fluorescence emission. We propose to use a 2D dielectric annular Bragg resonator [21,22] rather than plasmonic structures to enhance the fluorescence emission. Dielectrics have much less intrinsic materials losses than metals at optical frequencies, thus the quenching effect can be greatly suppressed. Meanwhile, we can still achieve considerable local excitation enhancement by properly designed dielectric structures.

The proposed dielectric ring resonator is schematically shown in Fig. 1(a). It consists of high-dielectric-constant concentric rings with optimized grating periodicity. In the experiment, the rings are made of titanium oxide whose refractive index is around 2.3 in the visible region. Due to the periodic gratings, incident light can be converted to in-plane guided waves, which are eventually concentrated at the center thanks to the constructive interference [12,15,23,24]. A small hole at the center can further confine and amplify the field arising from the strong dielectric contrast (titanium oxide versus water, see the following text), which is similar to the mechanism of slot waveguide modes [25]. Alternatively, the structure can be considered as a defect surrounded by radial Bragg reflectors. Such a circular resonator based on radial Bragg reflectors can achieve ultra-small modal volume and a large quality factor, and has been applied to realize single-mode lasing at room temperature [22]. Figure 1(b)

shows the scanning electron microscope (SEM) image of one fabricated annular Bragg resonator. The sample was fabricated using electron beam lithography on a quartz substrate whose surface is covered by a 2 nm layer of indium tin oxide (ITO). The titanium oxide film was obtained by reactive electron beam evaporation of Ti_3O_5 and a lift-off process was followed [26].

We perform numerical simulations based on commercial electromagnetic solvers (CST Microwave Studio and COMSOL Multiphysics) to verify the field enhancement of the proposed 2D ring cavities. The period, width, and height of the ring are 410 nm, 200 nm and 90 nm, respectively, and the diameter of the central hole is 100 nm. The ring is made of Ti_3O_5 ($\epsilon_{\text{Ti}_3\text{O}_5} = 5.29$ which is determined by ellipsometry measurement), the substrate is quartz ($\epsilon_{\text{quartz}} = 2.1$), and the surrounding medium is water ($\epsilon_{\text{water}} = 1.77$).

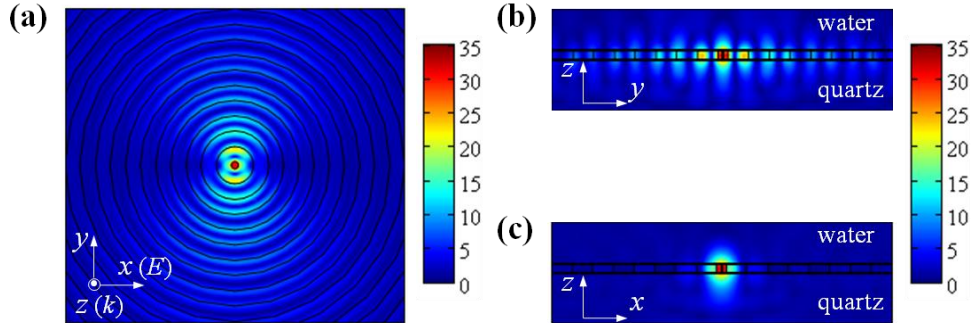


Fig. 2. The distribution of the electric field in the cavity at the wavelength of 640 nm. (a)-(c) plot the amplitude of the electric field ($|E|$) at three different cross-sections.

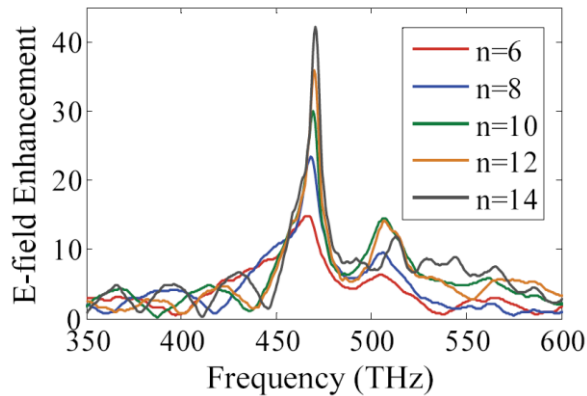


Fig. 3. The field enhancement at the center of the cavity for different numbers of rings.

Figure 2(a) plots the electric field distribution when a linearly polarized light (polarization along the x-axis) illuminates the ring cavity perpendicularly (that is, light propagates along the z-axis). Around the resonance condition, the concentric gratings diffract and convert the normal incident light to in-plane guided waves, which are constructively interference with each other. The field is eventually focused and enhanced at the center of the annular Bragg cavity. However, the x-polarized light cannot sense the periodicity of ring along the y-direction. Therefore, the field spreads in the y-direction, as shown in Figs. 2(b) and 2(c). Due to the cylindrical geometry, the eigenmodes of the system are radial modes characterized by different angular propagation indices. Annularly polarized incident light and precise modulation of the periodicity may further strengthen the field confinement [21,22]. Nevertheless, the absolute amplitude of the electric field can be still dramatically increased at the center of the current design, which is plotted in Fig. 3 for different numbers of periods.

One can see that the electric field, which is dominated by the x component, can be readily enhanced over 10 times with only 6 concentric rings. When the total number of rings is 14, the electric field at the center is more than 40 times larger than the incident field, implying the fluorescence emission can be increased more than three orders of magnitude at the resonance peak wavelength (see Eq. (1)). In addition, the sharp drop of the resonance peak after the maximum indicates the Rayleigh's cutoff phenomenon (the Wood's anomaly effect) [23,27]. It is possible to further narrow the spectral width of the resonance down to several nanometers [27], and thus the quality factor and field enhancement can be improved.

We have also simulated the plasmonic (silver) annular Bragg cavity with a similar geometry that operates at the same wavelength. Due to the interference and focusing of surface plasmons, the maximum field enhancement of the plasmonic resonator is about 21, which is half of the dielectric counterpart. To calculate the external quantum efficiency in the presence of metals, a dipole emitter is introduced at a certain position. By comparing the far-field radiation energy assisted by the resonator as well as the dissipated energy in the metal with respect to the radiation of the same dipole in free space [7], the external quantum efficiency for a local position can be obtained according to Eq. (2). Finally, we can calculate the fluorescence emission enhancement from Eq. (1). It is found that the emission enhancement factor for a dipole emitter placed at the resonator center is only 53, indicating that the quenching effect already starts to play a negative role. A more comprehensive comparison of the fluorescence emission enhancement between the dielectric annular Bragg cavity and the plasmonic one will be studied in the future and presented elsewhere.

3. Fluorescence experiments and discussions

Fluorescence enhancement measurement is a good way to characterize the field enhancement, and it is also a nice demonstration of the potential applications of such a cavity for chemical or biological sensors. Thus after the designed ring cavities had been fabricated, we incubated them with 200 $\mu\text{g/ml}$ APC (Allophycocyanin) conjugated IgG (from Ebioscience) for 20 hours at 4 degree. After careful rinses with deionized water for 3 times (1 hour each time), a uniform coating of fluorescent molecules was formed on the sample. We imaged the samples with Nikon TE2000 optical microscope using a 4x objective lens (0.13 N.A.), with the excitation band from 567.5 nm to 622.5 nm and detection band from 632.5 nm to 697.5 nm.

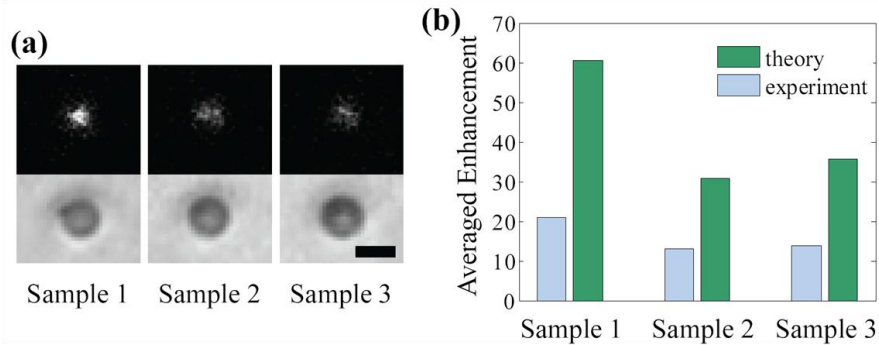


Fig. 4. (a) The fluorescence images of three different annular Bragg resonant cavities, exhibiting the maximum enhancement factors 21, 13, and 14, respectively. For the three samples, the width of the ring is fixed as 200 nm, the height of the ring is 90 nm, while the periodicity of sample 1, 2, 3 is 410 nm, 390 nm and 430 nm, respectively. The upper panel is the fluorescence enhancement images and the bottom panel is the corresponding bright field images. The scale bar is 20 μm . (b) The simulated averaged fluorescence enhancement over an area of 4 μm^2 at the central region of the cavity, in comparison with the experimental results.

The measured fluorescence enhancement images and the corresponding bright field images are presented in Fig. 4(a). The enhancement by annular Bragg resonant cavities can be clearly seen, while different enhancement factors were detected for three types of the cavities with varied periodicities. We quantitatively determined the fluorescence enhancement by

$$\eta = (I_{\text{sample}} - I_{\text{background}}) / (I_{\text{substrate}} - I_{\text{background}}) \quad (3)$$

where I_{sample} , $I_{\text{substrate}}$ and $I_{\text{background}}$ refer to the collected light intensity from fluorophores on annular Bragg resonator samples, fluorophores on the substrate and background noise signals of a bare substrate without fluorophores, respectively. The maximum enhancement factors for sample 1, 2, 3 were 21, 13, 14 respectively. It should be pointed out that we also did control experiments of the fluorescence enhancement of 1D dielectric Ti_3O_5 gratings with similar geometry parameters following the same experimental procedure. The fluorescence signals from 1D gratings strongly depend on the polarization of the illumination light [14]. For TM (TE) light with electric fields polarized perpendicular (parallel) to the gratings, the fluorescence on the grating area is clearly (barely) enhanced in comparison with that on the bare substrate (data not shown here). Such control experiments confirmed that the fluorescence enhancement was due to the field enhancement rather than fluorophore preferred nonspecific binding, which meant that the difference of fluorophore binding affinity between Ti_3O_5 and ITO, and thus the variation of fluorophore local density were neglectable.

The experimental results did not reach the predicted maximum enhancement at the center of the cavity, because the enhancement factor was significantly underestimated due to the following facts: First of all, a low N.A. lens was used to illuminate the sample almost perpendicularly, so that the illumination light could be efficiently coupled to the guided mode. On the other hand, the low N.A. lens limited the spatial resolution. Considering the pixel size of CCD used in the experiment, the fluorescence enhancement images in Fig. 4(a) in fact represented the averaged enhancement roughly over $4 \mu\text{m}^2$ sample area per pixel. Secondly, the fluorophores were linked with the antibodies before being coated to the sample. Because of the physical size of the antibodies, the APC molecules were about 5-10 nm from the sample surface on average, where the field enhancement was smaller than just at the surface of the sample. Taking into account these two factors, we performed numerical simulations and plotted the averaged enhancement factor over $4 \mu\text{m}^2$ in the central region of the cavity but 7.5 nm above the sample surface. One can see that the general trend agrees well between the experiment and simulation. The reasons for the 2-3 fold discrepancy may include: (1) The excitation and emission bands were around 60 nm in width respectively, thus the measured results should be an average of a certain width of enhancement peak in the spectrum around 640 nm; (2) The maximum enhancement was designed for normal incident light. Though we used a low N.A. objective lens in the experiment, the measured data were still of an average of incident light angle within 7.5 degree solid angle; and (3) the imperfection of the fabricated structures. Near-field mapping such as NSOM (Near-field Scanning Optical Microscopy) measurement in principle could provide direct information of the local field enhancement of the resonator with a better spatial resolution, but it is out of the scope of the current work.

4. Conclusions

We have demonstrated fluorescence emission enhancement by a two-dimensional dielectric annular Bragg resonant cavity. Due to the constructive interference of the in-plane guided wave around the resonance wavelength, the electric field can be focused and amplified considerably. Such a strong field leads to the significant fluorescence enhancement in the experiment. The observed maximum averaged enhancement is about 20 times over an area of $4 \mu\text{m}^2$, in a good agreement with the simulations. Our dielectric structures enable to avoid significant quenching of fluorescence. We envision that such dielectric ring cavity structure may have broad applications, ranging from near-field optical trapping, to ultrasensitive chemical and biological sensors, and to fluorescent microscopy at the single-molecule level.

Acknowledgements

This work was supported by the National Science Foundation (NSF) Nanoscale Science and Engineering Center (CMMI-0751621)